Meiotic recombination-related DNA synthesis and its implications for cross-over and non-cross-over recombinant formation

Masahiro Terasawa*, Hideyuki Ogawa*, Yasumasa Tsukamoto*, Miki Shinohara†, Katsuhiko Shirahige‡, Nancy Kleckner§¶, and Tomoko Ogawa*

*Iwate College of Nursing, Ohgama, Takizawa, Iwate 020-0151, Japan; †Institute for Protein Research, Osaka University, Suita, Osaka 565-0871, Japan; ‡Gene Research Center, Tokyo Institute of Technology, Nagatsuta, Midori-ku, Yokohama 226-8501, Japan; and §Department of Molecular and Cellular Biology, Harvard University, 7 Divinity Avenue, Cambridge, MA 02138

Contributed by Nancy Kleckner, January 12, 2007 (sent for review November 6, 2006)

Meiotic recombination-related DNA synthesis (MRDS) was analyzed in *Saccharomyces cerevisiae* by specifically timed incorporation of thymidine analogs into chromosomes. Lengths and positions of incorporation tracts were determined relative to a known recombination hot spot along DNA, as was the timing and localization of incorporation relative to forming and formed synaptonemal complex in spread chromosomes. Distinct patterns could be specifically associated with the majority cross-over and non-cross-over recombination processes. The results obtained provide direct evidence for key aspects of current consensus recombination models, provide information regarding temporal and spatial relationships between non-cross-over formation and the synaptonemal complex, and raise the possibility that removal of RecA homolog Rad51 plays a key role in regulating onset of MRDS. Finally, classical observations on MRDS in *Drosophila*, mouse, and lily are readily mapped onto the findings presented here, providing further evidence for a broadly conserved meiotic recombination process.

combing DNA | thymidine analogs | meiosis | MER3 | recombination tracts

An important role of meiosis is the mixing of parental genetic information, both by random segregation of maternal versus paternal versions of each chromosomes into progeny germ cells and by programmed DNA recombination. In most organisms, recombination also plays a mechanical role in ensuring regular segregation of homologs at the first meiotic division.

An integral feature of recombination should be local DNA synthesis in and around the site of each interaction. However, such meiotic recombination-related DNA synthesis (MRDS) has not been analyzed since the advent of molecular studies of meiosis, which have yielded specific recombination models and increased understanding of temporal, spatial, and functional relationships between DNA events and concomitant global changes along and between chromosomes. This study investigates these issues in budding yeast *Saccharomyces cerevisiae*. These results should be widely applicable: the biochemical events of recombination and their timing with respect to global chromosomal events appear to be conserved among many organisms, including budding yeast, several other fungi, mouse, human, and several plants.

In all studied organisms, recombination is initiated by the tightly regulated, meiotically specified occurrence of double-strand breaks (DSBs) catalyzed by the conserved transesterase protein Spo11 (1). Budding yeast studies reveal that DSB formation is accompanied by the tightly linked resection of 5′ strand ends to produce 3′ single-stranded tails. Genetic plus physical studies in many organisms further suggest that most initiating DSBs interact with the corresponding position on a (nonsister) chromatid of the homolog, rather than the sister chromatid (2, 3), and are processed in one of two alternative ways that lead to either a cross-over (CO) or a non-cross-over (NCO) product. In a CO, chromosome segments flanking the initiation site are exchanged between the homologs; in an NCO, there is no such exchange. The decision as to which path a DSB will follow is determined quite early in the process, before any stable/extensive (detectable) strand exchange (3–6).

Fig. 1 describes a current consensus model for meiotic recombination (e.g., refs. 3–5). Most DSBs that eventually mature into COs proceed to that fate by was of two successive discrete long-lived intermediates: single-end invasions (SEIs), in which one resected DSB end interacts with a partner duplex, and double-Holliday junctions (dHJs), which are fully covalently closed molecules in which both DSB ends have engaged the partner, and gaps corresponding to the resected portions of the two ends have been resynthesized. Resulting COs exhibit a unique spatial distribution, "interference," in which events tend not to occur near one another (7). Intermediates leading to the formation of NCO products have not been identified, but they likely occur by synthesis-dependent strand annealing (3–5). In some organisms, a few COs arise by a process that does not involve interference or, as shown for yeast, SEIs or dHJs. Several models for the origins of these COs have been proposed (3, 6, 8).

Recombinational progression occurs in close temporal correspondence to global changes in chromosome organization and juxtaposition of homologs (Fig. 1). DSBs occur at approximately early leptotene. Ensuing steps then occur during zygotene and pachytene, the stages at which homologs become, and then remain, tightly connected all along their lengths by means of the synaptonemal complex (SC). DSBs disappear at the leptotene/zygotene transition. Then, along the CO branch of the pathway, three discrete transitions occur. (*i*) DSBs are converted to SEIs during zygotene, concomitant with formation of SC; indeed, SC formation is likely nucleated preferentially or exclusively at the "CO-designated" sites where SEIs are forming in axis-associated recombination complexes (9). (*ii*) SEIs are converted to dHJs at midpachytene. (*iii*) dHJs are resolved into COs toward the end of pachytene. The timing of events along the NCO branch of the pathway is less clear (below). These relationships, documented most explicitly in yeast (10), are likely to be widely conserved as judged by cytological analysis of recombination proteins in several organisms and physical studies of DNA in mouse (e.g., refs. 11–13).

Author contributions: M.T., H.O., N.K., and T.O. designed research; M.T. performed research; M.S. and K.S. contributed new reagents/analytic tools; M.T., H.O., Y.T., N.K., and T.O. analyzed data; and M.T., H.O., Y.T., N.K., and T.O. wrote the paper.

The authors declare no conflict of interest.

Abbreviations: CO, cross-over; dHJ, double Holliday junction; DSB, double-strand break; MRDS, meiotic recombination-related DNA synthesis; NCO, non-cross-over; SC, synaptonemal complex; SEI, single-end invasion.

¶To whom correspondence should be addressed. E-mail: kleckner@fas.harvard.edu.

This article contains supporting information online at www.pnas.org/cgi/content/full/0611490104/DC1.

GENETICS

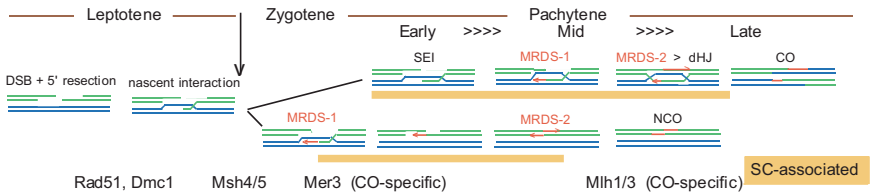

Fig. 1. Consensus model for meiotic recombination plus temporal and spatial relationships to forming and formed SC. Parental DNAs are represented by two green and two blue bars; MRDS are indicated by red bars with/without arrows. For green duplex, top strand is drawn 5′ to 3′ (left to right); for blue duplex, top strand is drawn 3′ to 5′ (left to right). Timing of events shown relative to classical meiotic stages (leptotene is equivalent to prophase before SC formation; zygotene are SC forming; pachytene are SC full-length). Also shown: (*i*) times when recombination intermediates are expected to be spatially associated with forming or formed SC (yellow underlining) and (*ii*) times of appearance of key recombination proteins (bottom line).

A final conserved aspect of meiotic recombination is that biochemical recombination complexes are physically associated with chromosome axes at many stages (refs. 11 and 14; Fig. 1). Association arises before or immediately after DSB formation, as seen by axis-association of RecA homologs Rad51 and Dmc1 (e.g., ref. 15), which load onto DSB ends (16). Thereafter, CO-designated interactions nucleate SC formation and retain their SC association for the entire recombination process, as seen through CO-correlated "pachytene nodules," and Mlh1/3 immunostaining foci. NCO-designated interactions, in contrast, may begin just before or just after SC formation (below), are SC-associated at early stages, and then appear to lose their SC during zygotene or early pachytene, as indicated by the kinetics and numbers of the corresponding nodules or immunostaining foci (e.g., refs. 11 and 17).

The consensus recombination model makes several specific predictions regarding the physical location(s) and lengths of newly synthesized DNA with respect to an initiating DSB site, the timing of synthesis during prophase, and the cytological localization of the corresponding recombination complexes with respect to forming or formed SC (Fig. 1; see below).

Here, specifically timed incorporation of thymidine analogs was used to examine occurrence of MRDS in relation to CO and NCO formation at the DNA level and in relation to the SC and recombination proteins by cytological studies. Taken together, the results presented provide a firm step toward establishing a fundamental understanding of meiotic recombination and its chromosomal context.

Results

A System for Efficient Incorporation of BrdU into Yeast Chromosomal DNA. The rapidly, synchronously sporulating *S. cerevisiae* SK1 strain NKY1551 was genetically modified to efficiently incorporate thymidine analogs (e.g., BrdU, IdU, and CldU) by addition of two facilitating genes: herpes simplex virus thymidine kinase (*HSV-TK*) and human equilibrative nucleoside transporter (*hENT1*) [*Materials and Methods*; and see supporting information (SI) Table 1]. When the resulting strain, MTY110, undergoes meiosis in the continuous presence of BrdU (400 μg/ml), incorporation of the analog is detectable by at t = 1 h, maximal by t = 2 h, and constant thereafter, as judged by antibody detection in a dot blot of extracted DNA (SI Fig. 8*A*). Comparison with a fully substituted control fragment generated by PCR suggests that BrdU is substituted for 1/5–1/3 of all thymine residues (data not shown). BrdU incorporation is specific to the genetically modified strain and does not affect meiotic progression as defined by timing of the meiosis I division (SI Fig. 8*B*).

MRDS Is Temporally and Functionally Distinguishable from Meiotic DNA Replication. BrdU incorporation was compared in MTY110 versus isogenic mutant derivatives expected to be defective in MRDS: *spo11*Δ and *rad50*Δ fail to make DSBs, *rad50S* blocks DSB resection, and *dmc1*Δ blocks immediate postresection steps. Meiotic cultures were pulse-labeled with BrdU at appropriate times (Fig. 2*A*) and then immediately harvested and examined for analog incorporation by immunostaining of surface spread chromosomes. Bulk DNA replication occurs between t = 0 h and t = 3 h in these conditions (18, 19). Correspondingly, in all five strains examined, pulses of incorporation from 0 to 2 h, or 2 to 3 h, yielded intense foci of BrdU located all along the chromosomes (Fig. 2*B*). In contrast, for pulses of incorporation at later times, WT cells exhibited discrete BrdU foci, whereas the several analyzed mutants did not (Fig. 2*B* and data not shown). Cells undergoing MRDS (given by subtracting the proportion of BrdU-positive *spo11*Δ nuclei from the proportion in WT) first appear at t = 3–4 h and become prominent at t = 4–5 and t = 5–6 h (Fig. 2*C*, red line). This timing matches the known progression of recombination in SK1 strains (10). Further, in *mer3*Δ, which is specifically defective in formation of COs, MRDS foci are rarer than in WT (Fig. 2*C*).

Importantly, in WT, the average number of BrdU foci per nucleus after pulse-labeling for samples 3–4 h, 4–5 h, and 5–6 h was 17, 23, and 15, respectively. However, when WT nuclei were continuously labeled for 3 h from 3 to 6 h, an average of 56 foci per nucleus in 146 nuclei was observed. This finding, plus the fact that the majority of the pulse-labeled nuclei show BrdU foci during all

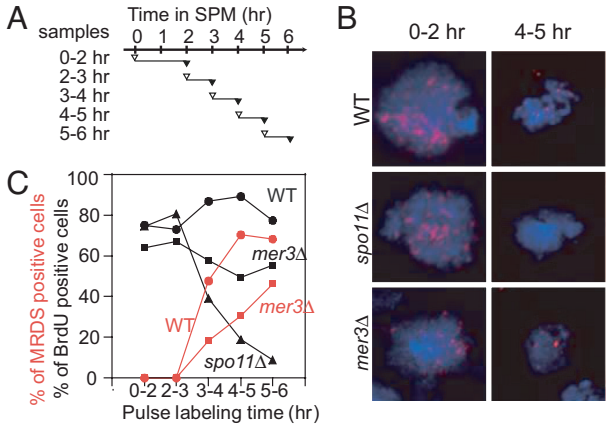

Fig. 2. Incorporation of BrdU in meiotic chromosomal DNA. (*A*) Pulse-labeling and sampling schedule for *B* and *C*. BrdU (200 μg/ml, open triangles) was added to cells undergoing synchronous meiosis at indicated time and harvested at the end of the labeling period (filled triangles). (*B*) Representative chromosomes labeled with BrdU. Wild-type, *spo11*Δ, and *mer3*Δ cells undergoing meiosis, incubated with BrdU during 0–2 or 4–5 h and harvested at 2 or 5 h, respectively. Chromosomes were spread on a glass slide at the indicated times and stained with anti-BrdU antibody (red) and a DNA-staining dye, YOYO-1 (blue). (*C*) Kinetics of BrdU incorporation by pulse-labeling in WT (filled circles), *spo11*Δ (filled triangles), and *mer3*Δ (filled squares) strains. At each time point, ≥100 nuclei containing >5 BrdU foci were counted. Percentage of MRDS-positive cells (WT, red circles; *mer3*Δ, red squares) calculated by subtracting percentages of BrdU-positive cells of *spo11*Δ from those in *SPO11 MER3* or *SPO11 mer3*Δ, respectively.

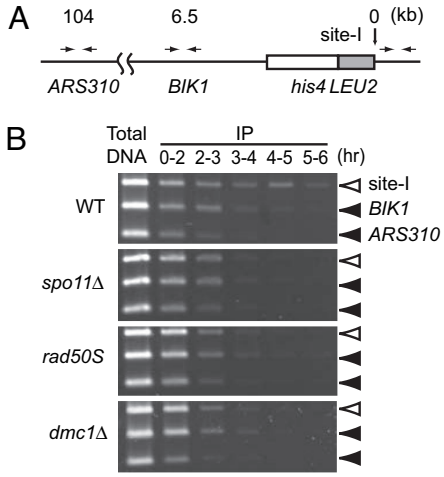

Fig. 3. Detection of MRDS at a recombination hot spot. (*A*) Map of sites examined. Horizontal arrow sets show primer locations versus distance from site I. (*B*) Detection of fragments incorporating BrdU by multiplex PCR of total and IP-DNAs with three primer sets in *A*. DNAs obtained from WT and mutant cells pulse-labeled as described in Fig. 2*A*.

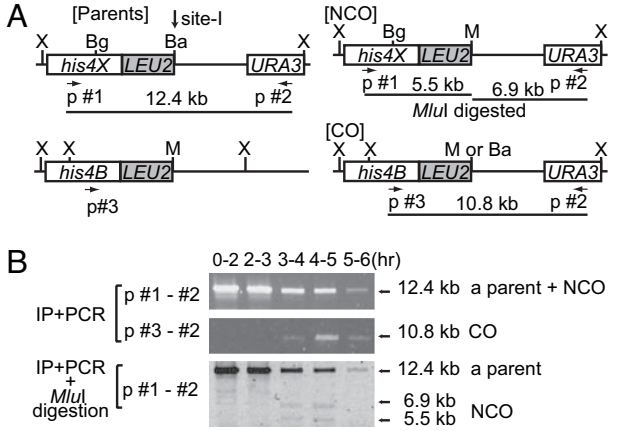

Fig. 4. Detection of BrdU-labeled CO and NCO recombinant molecules at site-I. (*A*) Restriction maps of two parental *his4LEU2* regions and locations of primers used (#1, #2, and #3). Lengths of PCR products shown by bars under the respective maps of [Parents], [NCO], and [CO]. Primer #1 hybridizes only to the *his4X* allele. Primer #3 hybridizes only to the *his4B* allele. A primer set comprising primers #1 and #2 amplifies both parental molecules and NCO recombinants. NCO molecules are detected by cutting products with restriction enzyme MluI. A primer set comprising primers #3 and #2 amplifies a CO recombinant. X, XhoI; M, MluI; Ba, BamHI; Bg, BglII; p, primer. (*B*) Gel patterns of CO and NCO recombinant molecules by PCR using IP-DNA.

three intervals, suggests that MRDS events occur at different times at different locations within an individual cell.

MRDS Occurs at a Recombination Hot Spot, Earlier in NCOs and Later in COs. Incorporation of BrdU was examined for products arising at a well characterized DSB hot spot, site I of the *his4LEU2* construct on chromosome III (20). Meiotic cultures of MTY110 and recombination-defective derivatives were pulsed appropriately with BrdU and immediately harvested. Genomic DNA was purified, sonicated, and immunoprecipitated with anti-BrdU antibody, and the immunoprecipitate (IP-DNA) was analyzed by PCR. Levels of BrdU-containing DNA were determined for a segment exactly adjacent to site I; a segment ≈6.5 kb away (*BIK1*) and a distant segment in a recombination-cold region (*ARS310*) (Fig. 3*A*). For S-phase pulse periods (0–2 h and 2–3 h), the relative abundance of IP-DNA at the three sites was constant in all four analyzed strains (Fig. 3*B*). During the recombination period (3–4 h, 4–5 h, and 5–6 h pulses), in WT cells, the abundance of IP-DNA increased at all three sites, with high levels at site I, intermediate levels at the adjacent locus and low levels at the cold spot. High levels of IP-DNA were also observed at a native DSB hot spot (*YCR047c* promoter; data not shown). In recombination-defective mutants, in contrast, no increase was observed (Fig. 3*B*).

IP-DNAs from pulse-labeled cells were also analyzed for the presence of CO and NCO recombination products at *his4LEU2* (Fig. 4*A*). Parental molecules were detected at all time points. NCO and CO molecules could be detected primarily at later time points. NCO recombinants are nearly maximal by 3–4 h; CO recombinant molecules are maximal only at 4–5 h (Fig. 4*B*). We infer that NCO products appear nearly an hour before CO products.

CO-Correlated MRDS Tracts Occur to Either Side of the Initiating DSB Site, Whereas NCO-Correlated MRDS Spans the DSB Site. Positions of MRDS tracts relative to an initiating DSB site, the lengths of such tracts, and their time of occurrence can all be directly examined by DNA-combing analysis. Molecules of interest were stretched uniformly on a coverslip stained with an appropriate antibody (or antibodies) to detect incorporated BrdU and concomitantly subjected to FISH with probes to the left arm of chromosome III (Fig. 5*A*). Simultaneous detection of four FISH probes of appropriate specific lengths and positions permitted identification of fully stretched molecules and, among these, the position(s) and length(s) of each MRDS signal (Fig. 5).

The distinction between MRDS and meiotic DNA replication was sharpened by using two antigenically distinguishable halogenated thymidine analogs. Wild-type cells were incubated for 3 h in sporulation medium (SPM) containing IdU to label meiotic DNA replication and then washed, immediately resuspended in medium containing CldU, and further incubated to the end of meiosis ($t = 8$ h), to label MRDS tracts. As expected, IdU foci were distributed along the chromosomes (Fig. 5*B* 1–6, green foci), whereas CldU foci were found at limited sites (Fig. 5*B* 1–4, red foci). Among 65 FISH- and IdU-positive fibers analyzed, 33 contained one or two CldU foci (total = 37). As expected for MRDS, these foci are positioned among continuously distributed IdU foci and occur preferentially around the site I DSB hot spot and the weaker nearby hot spot, site II (Fig. 5*B* and SI Fig. 9*A*). Also, in parallel analysis of *spo11*Δ cells, no CldU foci were observed among such fibers (Fig. 5*B* 5 and 6; also SI Table 2).

Among 35 fibers with FISH hybridization at sites flanking *his4LEU2*, 22 had MRDS tracts localized at or near site I or site II. Among these, 15 extended to only one side of a DSB site (Type I; Fig. 5*C*, red bars) and 7 extended to both sides of a site (Type II; Fig. 5*C*, blue bars). Additionally, 10 fibers contained incorporation in the hot spot region but with endpoints removed from the DSB site, and three contained very long tracts (Fig. 5*C*, black bars).

Type I and Type II MRDS tracts are precisely those predicted by current models for CO- and NCO-related recombination, respectively (Fig. 1). Modulations of these models (3) can explain the other 10 hot spot-associated tracts. Other expectations are also confirmed. First, both products of a CO event should contain MRDS, whereas only one of the two products of an NCO event contain MRDS (Fig. 1). Thus, the predicted ratio of CO to NCO events as inferred from fiber analysis would be ≈1:1 [15:(7 × 2)]. This matches the ratio observed directly at this site (21). Second, *mer3*Δ reduces CO recombination by 2/3 in the current conditions (22). Here, *mer3*Δ reduces the fraction of Type I fibers and increases the fraction Type II fibers (to 5 of 29

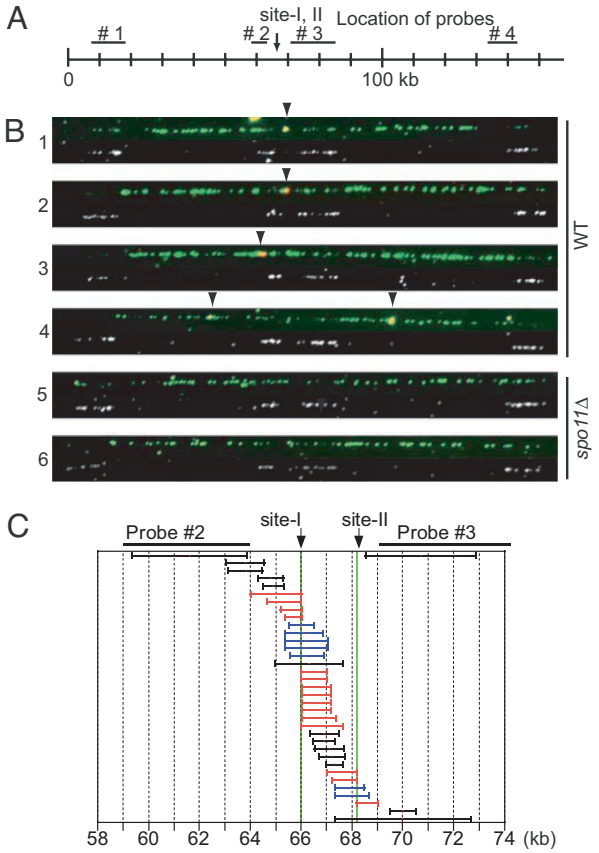

Fig. 5. Locations of MRDS tracts on combed DNA. (*A*) Map of chromosome III, left arm in kb from left end (equal to 0 kb). Arrow indicates sites I+II. Bars #1–4 show locations of probes. (*B*) Combed DNA incorporating IdU and CldU in WT and *spo11*Δ strains (representative patterns). (*B* 1–6 *Upper*) IdU and CldU foci. (*B* 1–6 *Lower*) Foci of four FISH probes. Arrows mark CldU foci. (*C*) Location and lengths of tracts of MRDS around site I and site II on WT DNA. Positions of CldU foci localized between probes #2 and #3 determined as distance from right edge of probe #2, normalized to the total distances between the two probes. Red bars indicate signals that locate at either side of site I or II. Blue bars indicate signals that span the sites.

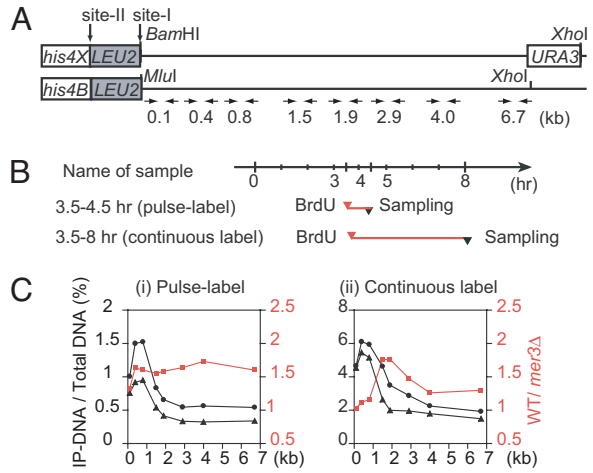

Fig. 6. MRDS tract lengths in WT and *mer3*Δ cells. (*A*) Locations of eight primer sets on the right side of site I at *his4LEU2*. (*B*) BrdU labeling and sampling schedule. Cells labeled with 200 μg/ml of BrdU for either 3.5–4.5 h (pulse labeling) or 3.5–8 h (continuous labeling). (*C*) The number of fragments incorporating BrdU was obtained by amplifying DNA from WT (filled circles) and *mer3*Δ (filled triangles) cells by PCR. Recovery of IP-DNA (%) equals the amount of PCR product of IP-DNA divided by the amount of total DNA. The ratio of WT to *mer3*Δ recovery in each sample is shown against distance from site I for the three labeling conditions (red line, filled squares).

and 13 of 29, with 11 of 29 uninformative), with a resulting predicted CO/NCO ratio of ≈1:5 [5:(13 × 2)], and an inferred reduction in COs to 20% of the WT level (SI Fig. 9*B*). Third, tract patterns match results of heteroduplex DNA studies showing that coconversion of markers located 300 and 600 bp to the "left" and "right" of a DSB hot spot is very rare (23).

Taken together, these results provide strong support for the notion that CO recombination occurs via the SEI/dHJ pathway, whereas NCO recombination occurs via the synthesis-dependent strand annealing pathway, with MRDS at the positions predicted by detailed versions of these models (Fig. 1).

MRDS Tracts of CO Recombination Are Longer and Occur Later than Those of NCO Recombination. In the fibers discussed above, CldU regions for WT cells ranged in size from 0.7 to 5.3 kb, with a peak at ≈1–2 kb; in contrast, in a *mer3*Δ strain, where CO recombination is specifically reduced, average tract lengths are also significantly reduced (SI Fig. 9 *C* and *D*). We infer that NCO recombination involves shorter MRDS tracts than CO recombination. High-resolution mapping of MRDS confirms this conclusion. Wild-type and *mer3*Δ cells were labeled with BrdU from 3.5 to 8 h, to again label all MRDS regions (Fig. 6*B*). DNA was then isolated, sonicated to an average of 0.5 kb (shorter than the expected MRDS tract length), precipitated with anti-BrdU antibody, and IP-DNA subjected to PCR analysis with primers that detect 100- to 400-bp segments located 0.1, 0.4, 0.8, 1.5, 1.9, 2.9, 4.0, and 6.7 kb to the right of site I (Fig. 6*A*). All primer pairs gave similar amplification efficiencies for total DNA (data not shown). A strong peak of MRDS tracts occurred at 0.4–0.8 kb in both strains. In contrast, longer tracts were present in WT but essentially absent in *mer3*Δ, with a maximum differential at 1.5–1.9 kb (Fig. 6*Cii*). Thus, CO-related MRDS tracts are longer than NCO-related tracts. These results match analogous inferences from genetic studies in yeast, mouse, and human (13, 23, 24).

Temporal analysis of recombination predicts that MRDS should occur significantly earlier during NCO recombination than CO recombination (Fig. 1). To test this prediction, high-resolution PCR analysis was performed on DNA from cells specifically labeled with BrdU early in the recombination period, 3.5–4.5 h (Fig. 6*B*). Lengths of these early MRDS tracts peaked at 0.4–0.8 kb and decreased drastically at 1.5 kb, essentially identically in WT and *mer3*Δ IP-DNAs (Fig. 6*Ci*). We infer that CO-correlated MRDS tracts, which are longer and *MER3*-dependent, are absent at early times and thus appear later than NCO-correlated tracts, which are shorter and *MER3*-independent.

Finally, the absolute lengths of MRDS tracts related to CO and NCO recombination, ≈1.9 and ≈0.8 kb, respectively, fit well with those predicted from genetic studies (see above). Also, appropriately, minimum MRDS tract lengths correspond to the lengths of single-strand tails formed at DSB sites, ≈600 nt (25).

MRDS Tracts Occur During Zygotene, in Synapsed and Unsynapsed Regions, and During Pachytene, on and off the SC. CO-related MRDS, which occurs at the SEI-to-dHJ transition, should occur at midpachytene; NCO-related MRDS, in contrast, should first appear at the time of DSB disappearance, and thus during zygotene; a second phase of NCO-related MRDS should then occur later, concomitant with detection of NCO products, and thus during early pachytene (Fig. 1). Further, CO-related MRDS is strongly predicted to occur in SC-associated recombination complexes (see Introduction). Localization of NCO-related MRDS is less specifically predictable (see below).

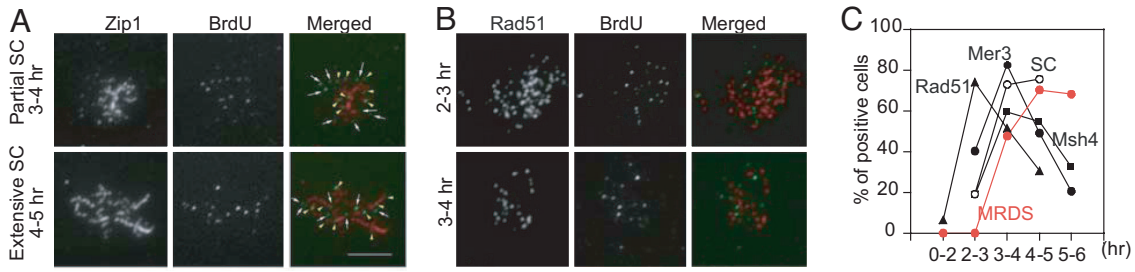

Fig. 7. Localization of BrdU foci relative to Rad51, Zip1, Msh4, and Mer3 foci. (*A*) Representative chromosomes with Zip1 and BrdU foci. Pulse-labeling of WT cells with BrdU carried out as in Fig. 2*A*. After 3- to 4-h, or 4- to 5-h pulse-labeling in meiosis, cells were harvested, chromosomes spread on a glass slide, and stained first with anti-Zip1 antibody (red in merged) and then with anti-BrdU antibody (green in merged). Yellow arrowheads in merged represent BrdU foci colocalized with Zip1. Arrows in merged represent BrdU foci that did not colocalize with Zip1. (Scale bar, 5 μm.) (*B*) Representative chromosomes stained successively with anti-Rad51 antibody (red in merged) and anti-BrdU antibody (green in merged). (*C*) Appearance of SC (open circles), and of Rad51 (filled triangles), Mer3 (filled circles), and Msh4 (filled squares) foci and of MRDS foci (red circles). MRDS was calculated as in Fig. 2*A*. Percentage of SC equals the number of partial and extensive SC cells divided by the number of Zip1-positive cells. The percentages of focus-positive cells equals the percentage of nuclei exhibiting >5 Rad51, Mer3, or Msh4 foci.

To investigate these issues, meiotic cells were pulse-labeled with BrdU at relevant time points and then immediately examined by BrdU immunostaining in surface spread preparations (Fig. 7*A*). Zygotene and pachytene nuclei contain partial and extensive SC, respectively. Percentages of the two types, defined by immunostaining of SC central region component Zip1, were: t = 2–3 h, 20% and 0%; t = 3–4 h, 31% and 42%; t = 4–5 h, 0% and 46%. Thus, as expected, CO-related MRDS, which occurs only after 3.5–4.5 h (above), must be occurring in pachytene nuclei, whereas, in contrast, by that same time, NCO-related MRDS has appeared not only in tracts but in mature products (Fig. 2), implying formation during zygotene/early pachytene.

Costaining of Zip1 and BrdU identifies zygotene and pachytene nuclei containing prominent foci with the moderate staining intensity specifically diagnostic of MRDS and with no evidence of very bright foci diagnostic of bulk DNA replication (above). Among BrdU foci in zygotene nuclei, about half colocalized with Zip1 on chromosomes in synapsed regions, whereas the remainder occurred unsynapsed region, i.e., where SC has not yet formed. In pachytene chromosomes, ≈60% of BrdU foci colocalized with Zip1/SC, whereas the remainder did not. Because CO-correlated foci are always SC-associated, we infer that non-SC-associated foci at zygotene and pachytene correspond to NCO recombination and, specifically, the two phases of MRDS (Fig. 1). If so, two new conclusions emerge. First, the first phase of NCO-related MRDS often occurs before and independent of SC formation. By implication, CO/NCO differentiation and interference can/often precede(s) SC polymerization across the corresponding locus (*Discussion*). Second, NCO-related recombination nodules disappear by early pachytene, an event that presumptively corresponds to release of DNA recombination complexes from association with the SC. Thus, the second phase of NCO-related MRDS appears to often occur concomitant with or after release of NCO complexes from the SC.

Rad51 Exits Most Recombination Complexes Before MRDS. Rad51 protein binds single-stranded DSB "tails." Rad51 immunostaining foci are most prominent during mid to late leptotene and zygotene (e.g., refs. 16 and 26). Simultaneous visualization of Rad51 and MRDS (Fig. 7*B*) reveals that (*i*) Rad51 foci appear before MRDS and (*ii*) when MRDS begins to appear, at t = 3–4 h, the fraction of Rad51-positive cells and the mean number of Rad51 foci per cell concomitantly begin to decrease. Moreover at this time, 80% of BrdU foci do not colocalize with Rad51 foci. We infer that Rad51 works most actively on DNA before MRDS occurs and that Rad51 leaves the sites of recombination before or shortly after initiation of MRDS. Because colocalization is very rare at all time points, this conclusion likely applies to both CO- and NCO-fated interactions. In contrast, foci of Msh4 and Mer3, two proteins involved in later stages of recombination (Fig. 1), appear and disappear successively, after Rad51 foci, and are roughly contemporaneous with MRDS foci (Fig. 7*C*). Also, extensive colocalization is observed for MRDS/Mer3, MRDS/Msh4, and Mer3/Msh4 (SI Figs. 10 and 11).

Discussion

The results presented above provide an examination of MRDS after 20 years. They permit definitive conclusions regarding the specific nature of CO- and NCO-related recombination, provide data regarding the spatial and temporal relationships between NCO recombination and the state of the SC, point suggestively to a key role for Rad51 in regulating the onset of recombination-associated synthesis, and permit the drawing of further analogies among the details of recombination-related events in diverse organisms.

CO Recombination. The observations presented directly confirm three specific features of the current consensus model for CO recombination (Fig. 1; see above): First, CO-related MRDS often extends from exactly the site of the initiating DSB outward, in both directions, to one side on one CO product and to the other side on the other CO product. Second, CO-related MRDS involves relatively long tracts of incorporation (1.5–1.9 kb). Third, CO-related MRDS occurs during pachytene and thus during the SEI-to-dHJ transition and in accord with its occurrence in SC-associated recombination complexes analogous to "pachytene/late recombination nodules." Our data also suggest that the first phase of NCO-related MRDS is often not spatially associated with developing SC. This result supports other types of emerging evidence that CO/NCO differentiation, and thus CO interference, occurs before and independent of SC polymerization (4, 6, 7, 27).

NCO Recombination. The current findings support four specific predicted features of NCO recombination by means of synthesis-dependent strand annealing (Fig. 1; see above). First, MRDS occurs to both sides of the initiating DSB site, but on only one of the two participating molecules. Second, NCO-related MRDS tracts are shorter than CO-related MRDS (≈0.8 kb). Interestingly, a C-terminal-truncated yeast *POL3* mutation specifically reduces CO formation and exhibits only short meiotic gene-conversion tracts (28). Perhaps Polδ is involved in CO-related MRDS. Third, NCO-related MRDS first appears earlier than CO-related MRDS, at zygotene, and thus during DSB disap-

pearance. Fourth, a second phase NCO-related MRDS should occur later than the first, i.e., at pachytene.

We also find that the NCO recombinant appears earlier than the CO recombinant, possibly during early to mid pachytene, when the corresponding recombination complexes are released from the SC. This appears to be an important general trend. In yeast, CO and NCO products may appear at the same time (29), but often NCO products precede CO products (5, 6); and NCOs appear before COs also in mouse (13).

Is Rad51 a Gatekeeper for Onset of MRDS? Our results suggest that exit of Rad51 from recombination complexes usually precedes MRDS. Perhaps Rad51 exit is essential for onset of DNA synthesis, e.g., because release from a Rad51 filament of single-stranded 3′ DNA at DSB end(s) is required for polymerase association. The two ends of a DSB are processed differentially, with differential loading of meiotic (Dmc1) and mitotic (Rad51) RecA homologs to the two ends potentially playing a key role (10, 30, 31). Thus, exit of Rad51, and perhaps also Dmc1, before and prerequisite to MRDS, could be a key element in ensuring an orderly sequential series of different biochemical processes at the two DSB ends.

Generality of MRDS Patterns Among Many Organisms. This study is preceded by classic studies of MRDS in *Drosophila*, mouse, and lily. Carpenter (32) demonstrated the occurrence of DNA synthesis at sites of SC-associated late (CO-correlated) recombination nodules in *Drosophila* by EM autoradiography. This observation is now clearly interpretable as synthesis during the SEI to dHJ transition. Moses and colleagues (33), using EM autoradiography of spread mouse chromosomes, identified significant DNA synthesis both during zygotene, with preferential localization along unsynapsed axes and atop the SC, and during pachytene, with especially extensive synthesis at discrete SC-associated positions plus additional less-extensive non-SC-associated synthesis. These patterns, qualitatively identical to the yeast situation above, can be similarly interpreted, with zygotene synthesis and non-SC-associated pachytene synthesis attributed to NCO-related recombination and extensive SC-associated synthesis at pachytene with the CO-related SEI-to-dHJ transition. Finally, in lily, Stern and Hotta (34) identified prominent synthesis of DNA of high sequence complexity, as expected for MRDS, specifically during pachytene (p-DNA), now attributable to CO-related and second-phase NCO-related synthesis. Zygotene MRDS was not reported for lily, but may have been obscured by synthesis of low-complexity sequences (zyg-DNA) whose origin is still unknown. Thus, MRDS studies support many other suggestions (e.g., refs. 1, 3, and 11) that the detailed mechanism of meiotic recombination, and its timing and localization with respect to forming and formed SC, is strongly conserved among many organisms.

Materials and Methods

To construct haploid SK1 strains containing the *HSV-TK* and *hENT1* genes, plasmid c3121 (*GPD-TK*) (35) and pKS007 (*ADH1-hENT1*) were integrated into strains NKY1331 and NKY1542 to produce strains MTY087 and MTY102, respectively. The resultant haploid strains were mated to yield the diploid strain MTY110. To construct plasmid pKS007, the *hENT1* gene was amplified (36) and cloned into a pAUR123 vector (TAKARA).

Meiotic chromosomes for spreading were prepared as described in Bishop (16). For assay of MRDS tracts by PCR, the immunoprecipitated yeast DNA with anti-BrdU antibody were subjected to the methods as described in Pichler *et al.* (37), with some modifications. For combing analysis, IdU, CldU, and probes were detected as described in Anglana *et al.* (38) with some modifications. For details, see *SI Materials and Methods*.

We thank Drs. Michael Lichten, Akira Shinohara, Neil Hunter, and Jun-ichi Tomizawa for discussion and critical reading; Ms. Y. Fujikawa for technical assistance; and Drs. A. Shinohara (Institute for Protein Research, Osaka University, Osaka, Japan), G. S. Roeder (Yale University, New Haven, CT), and T. Nakagawa (Osaka University School of Science, Toyonaka, Osaka, Japan) for generously providing antibodies. This work was supported by Grant-in-Aid for a Specially Promoted Research 14780530 (to T.O.); Grant-in-Aid for Young Scientists 1770150 (to Y.T.); National Institutes of Health Grant R01-GM44794 (to N.K.); and Exploratory Research Grant 17657058 from the Ministry of Education, Science, Sports, and Culture of Japan (to M.T.).

1. Keeney S (2001) *Curr Top Dev Biol* 52:1–53.
2. Schwacha A, Kleckner N (1997) *Cell* 90:1123–1135.
3. Hunter N (2007) in *Homologous Recombination*, eds Aguilera A, Rothstein R (Springer, Heidelberg).
4. Bishop DK, Zickler D (2004) *Cell* 117:9–15.
5. Allers T, Lichten M (2001) *Cell* 106:47–57.
6. Börner GV, Kleckner N, Hunter N (2004) *Cell* 117:29–45.
7. Jones GH, Franklin FC (2006) *Cell* 126:246–248.
8. Hollingsworth NM, Brill SJ (2004) *Genes Dev* 18:117–125.
9. Henderson KA, Keeney S (2005) *BioEssays* 27:995–998.
10. Hunter N, Kleckner N (2001) *Cell* 106:59–70.
11. Zickler D, Kleckner N (1999) *Annu Rev Genet* 33:603–754.
12. Moens PB, Kolas NK, Tarsounas M, Marco E, Cohen PE, Spyropoulos B (2002) *J Cell Sci* 115 (Pt 8):1611–1622.
13. Guillon H, Baudat F, Grey C, Liskay RM, de Massy B (2005) *Mol Cell* 20:563–573.
14. Blat Y, Protacio R, Hunter N, Kleckner N (2002) *Cell* 111:791–802.
15. Tarsounas M, Morita T, Pearlman RE, Moens PB (1999) *J Cell Biol* 147:207–220.
16. Bishop DK (1994) *Cell* 79:1081–1092.
17. Stack SM, Anderson LK (1986) *Chromosoma* 94:253–258.
18. Padmore R, Cao L, Kleckner N (1991) *Cell* 66:1239–1256.
19. Borde V, Goldman AS, Lichten M (2000) *Science* 290:806–809.
20. Cao L, Alani E, Kleckner N (1990) *Cell* 61:1089–1101.
21. Martini E, Diaz RL, Hunter N, Keeney S (2006) *Cell* 126:285–295.
22. Nakagawa T, Ogawa H (1999) *EMBO J* 18:5714–5723.
23. Jessop L, Allers T, Lichten M (2005) *Genetics* 169:1353–1367.
24. Jeffreys AJ, May CA (2004) *Nat Genet* 36:151–156.
25. Bishop DK, Park D, Xu L, Kleckner N (1992) *Cell* 69:439–456.
26. Terasawa M, Shinohara A, Hotta Y, Ogawa H, Ogawa T (1995) *Genes Dev* 9:925–934.
27. Page SL, Hawley RS (2004) *Annu Rev Cell Dev Biol* 20:525–558.
28. Maloisel L, Bhargava J, Roeder GS (2004) *Genetics* 167:1133–1142.
29. Storlazzi A, Xu L, Cao L, Kleckner N (1995) *Proc Natl Acad Sci USA* 92:8512–8516.
30. Shinohara M, Gasior SL, Bishop DK, Shinohara A (2000) *Proc Natl Acad Sci USA* 97:10814–10819.
31. Neale MJ, Keeney S (2006) *Nature* 442:153–158.
32. Carpenter AT (1981) *Chromosoma* 83:59–80.
33. Moses MJ, Dresser ME, Poorman PA (1984) *Symp Soc Exp Biol* 38:245–270.
34. Stern H, Hotta Y (1974) *Genetics* 78:227–235.
35. Lengronne A, Pasero P, Bensimon A, Schwob E (2001) *Nucleic Acids Res* 29:1433–1442.
36. Vernis L, Piskur J, Diffley JF (2003) *Nucleic Acids Res* 31:e120.
37. Pichler S, Piatti S, Nasmyth K (1997) *EMBO J* 16:5988–5997.
38. Anglana M, Apiou F, Bensimon A, Debatisse M (2003) *Cell* 114:385–394.